

amplitude enhancement occurring as a result of the application of a third weak forcing with a frequency tuned to the difference frequency generated by the original applied forcings. Through this process, one may therefore achieve a resonancelike behavior from an off-resonance spectral position. This first-time observation, potentially leading to novel dynamic multifrequency force microscopy, has not been previously reported.

In MSAFM, both the sample and the probe receive external elastic energy from piezoelectric substrates that are driven by voltage waveform generators giving rise to primarily transversal forces. Within the framework of continuum mechanics, Hamilton's extended principle may thus be employed to obtain the partial differential equation for the elastic wave propagation in the microcantilever (length L , density ρ , Young's modulus E , moment of inertia I , and tip mass m_e) shown in Fig. 1. Here, we aim to numerically show (a) how ω_- oscillations emerge when tuning the power form of the interaction force and (b) how these oscillations compare to measurements. Noting the transformation $\bar{r} = \bar{r}_{o'} + \bar{r}'$, $t = t'$, and setting $\bar{r}_{o'} = [0, h(t), 0]$, the action $\int_{t_1}^{t_2} (\delta T - \delta U + \delta W) = 0$, where the integrand is the sum of the variations in the kinetic energy T , the potential energy U , and the virtual work W , yields the partial differential equation (PDE) of the probe in the form:

$$\rho u_{tt}(x, t) + \rho h_{tt}(t) + E I u_{xxxx}(x, t) + c u_{xt}(x, t) = 0,$$

subject to the boundary conditions $u(0, t) = u_x(0, t) = u_{xx}(L, t) = 0$, and

$$m_e u_{tt}(L, t) + m_e h_{tt}(t) - E I u_{xxx}(L, t) = \Gamma(t), \quad \forall t,$$

where a general time dependent interaction force $\Gamma(t)$, to be specified, and a structural damping c have been assumed in writing the virtual work, and the applied excitation at $\bar{r}_{o'}$ has been incorporated in writing the kinetic energy. If we now assume that $\bar{r}_s = \bar{a}_s \sin(\omega_s t + \varphi_s)$ collectively represents the dynamics of the sample (with the forcing at $y = 0$) and any internal scattering of the ensuing elastic waves within the interior of the sample, for example, as a result of an embedded particle, then the probe-sample distance $d(t) = |\bar{r}_L - \bar{r}_s| = u(L, t) + h(t) - h_s(t)$, being modulated in time, may be used to express the spatial dependence of the interaction force $\Gamma(y, t)$. Subjecting the gap distance to the condition $d(t) \geq d_0 > 0$, we propose the semiempirical interaction force $\Gamma(t) = a_a d(t)^{\gamma_a} + a_r d(t)^{\gamma_r}$, with $a_a > 0$ and $a_r < 0$. To solve the resulting nonlinear, nonautonomous PDE, we employ an eigenfunction expansion (assumed mode) method [11]. Being a Galerkin approximation, this approach effectively casts the PDE into a discrete form appropriate for numerical analysis. Thus, homogenizing the boundary condition above via the variable substitution $u(x, t) = \zeta(x, t) + \Gamma(t)g(x)$, where $\beta g(x) = 2x^4 - 5Lx^3 + 3L^2x^2$, $0 \leq x \leq L$ is a geometrical function ($\beta = -18EIL$), and ex-

anding $\zeta(x, t) = \sum_{i=1}^n \phi_i(x)q_i(t)$, where $\phi_i(x)$ are the eigenfunctions of the probe while $q_i(t)$ are the generalized coordinates, we can express the interaction force as

$$\begin{aligned} \Gamma(t) = & a_a \left[\sum_{i=1}^n \phi_i(L)q_i(t) + \Gamma(t)g(L) + h(t) - h_s(t) \right]^{\gamma_a} \\ & + a_r \left[\sum_{i=1}^n \phi_i(L)q_i(t) + \Gamma(t)g(L) + h(t) - h_s(t) \right]^{\gamma_r}. \end{aligned} \quad (1)$$

We seek the power spectral density of the system $S(\omega) = |\mathcal{F}\{S(t)\}|^2$, with $S(t) \propto u(x_r, t)$, where x_r is the readout segment of the probe (Fig. 1).

Denoting the oscillation wavelength corresponding to an excited eigenmode with λ_{cr}^κ , $\kappa = 1, 2, \dots$, and that of a nonresonant mode with λ_{cu} , we begin a MSAFM session by imposing a forcing F_c at $\bar{r}_{o'}$ through $h(t) = a_{cu} \sin(\omega_{cu}t + \varphi_{cu})$, and another at $y = 0$. After a preliminary tuning of both frequencies ω_{cu} and ω_s , the feedback is invoked to maneuver the probe in the spatial regime where interatomic forces are active. Under these conditions, that is, when $d(t)$ is modulated, the discontinuous probe response as a function of the probe-substrate distance (force curve) is shown in Fig. 2, where the z position from which ω_- is studied has been marked. Considering the probe oscillation at the difference frequency to constitute a synthesized mode, the result in Fig. 2 shows that the amplitude is maximum when the z position corresponds to the probe just leaving the surface. To explain the formation of this new mode, as the amplitudes of the two applied forcings are continuously increased, we calculate the probe oscillation amplitude at the spectral position ω_- in the Fourier space. By studying the pair (γ_a, γ_r) , determining the power law of $\Gamma(t)$, the emergence of oscillations at ω_- is shown in Fig. 2 exhibiting an optimization for $(\gamma_a, \gamma_r) = (-2, -8)$ corresponding to the volume integrated Lennard-Jones potential [11,12]. The computed ω_- oscillation amplitude shows a higher sensitivity to the long-range van der Waals power form than the short-range repulsive power form, which, once turned on at $\gamma_r \leq -8$, exhibits little variation. Thus, frequency difference generation appears to more crucially depend on the particular power law of the long-range forces and does not appear for values outside $\gamma_a = -2 \pm \epsilon$, where ϵ is small. The result suggests that any nanoscale processes that may, in an effective manner, modify the repulsive form in the $\gamma_r < -8$ regime will not prevent ω_- generation.

In order to further examine the frequency difference generation by Γ , we choose to simulate the amplitude of ω_- oscillations in the parameter space spanned by (ω_{cu}, ω_s) and compare the result with that obtained experimentally. Lock-in detection of $S(t)$ referenced at ω_- over a mesh of $(\omega_{cu,i}, \omega_{s,j})$, $i = j = 1, 2, \dots, N$ is shown in Fig. 3. While the islands corresponding to ω_- generation in the simulated case appear more well separated than the experimental case, which includes smearing effects associated with the detector and electronic bandwidths

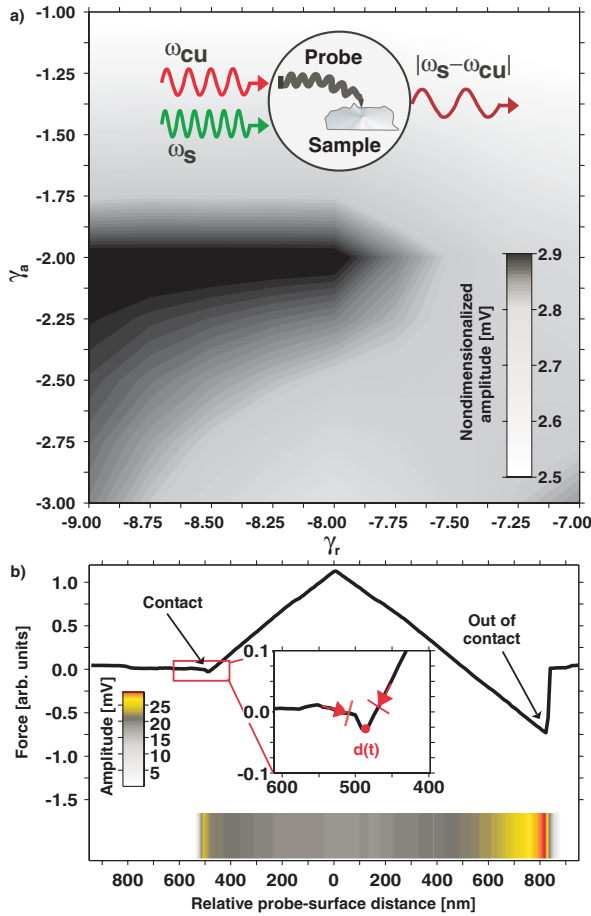


FIG. 2 (color online). Behavior of nanomechanical frequency difference generation. (a) Numerical simulation of the semi-analytical result obtained for the amplitude of oscillation at the difference frequency exhibited by the system shown in the inset, as a function of the form of Γ . (b) Experimental measurement of the distance dependence d of the force (solid curves) and the simultaneously detected amplitude of oscillation at the difference frequency (contour) for a given set of excitations $\omega_{cu} = 4.00$ MHz and $\omega_s = 4.38$ MHz yielding a peak $\omega_- = 380$ kHz, close to the third resonance of the probe.

and nonflat piezoelectric crystals' spectral response and signal noise, the trends are similar in both cases.

The measurement of the generated ω_- was sampled at several points along the force curve of Fig. 2 in the range from the point when the probe first contacts the surface to the point when it loses contact. While exciting the probe, a soft gold coated silicon nitride triangular cantilever of spring constant $k = 0.06$ N/m, and the sample, a freshly cleaved mica substrate, at 4.00 and 4.38 MHz with $a_s = a_p = 2$ V peak to peak, the distance $r_s - r_L$ is varied using the force curve mode of the AFM. Simultaneously, the evolution of ω_- amplitude is measured using a lock-in amplifier. Figure 2 provides the distance dependence of the ω_- generation suggesting the possibility of enhancing the signal by working in a configuration where the attractive forces are predominant (i.e., closer to the jump out of contact position). Clearly, no coupling can be observed

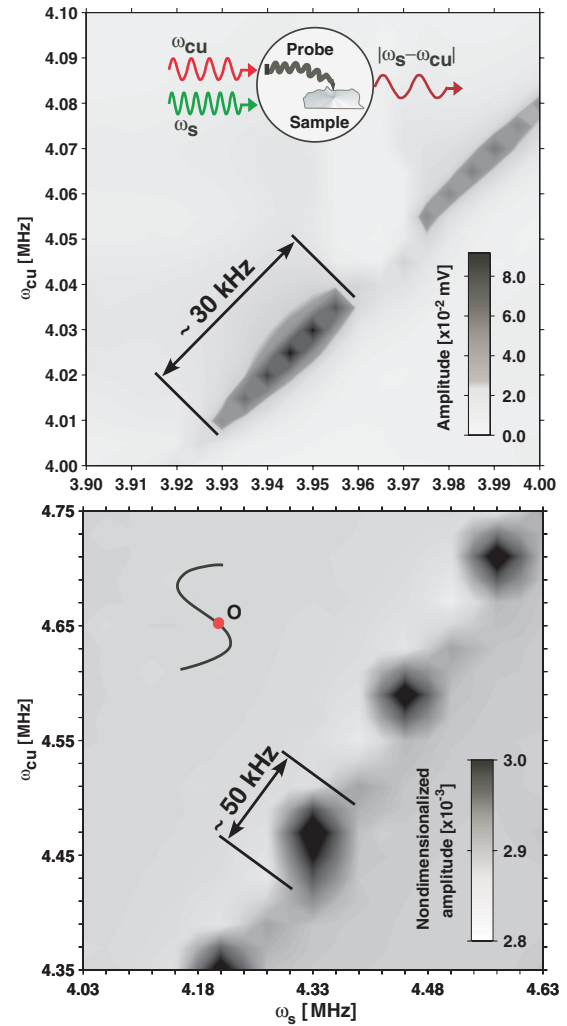


FIG. 3 (color online). Comparison between the experimental measurement (top) and theoretical modeling (bottom) of the oscillations at the difference frequency exhibited by the nonlinear system depicted by the inset. For this two stimuli case, an operational point (ω_s, ω_{cu}) may trace out an arbitrary path in the frequency domain when carrying out multiple measurements. The result presented in Fig. 4 may be obtained from any point O of one such typical trace in the off-resonance region.

before the probe tip jumps into contact and after it jumps out of contact with the sample surface. The gradient presented in Fig. 2(b) shows the enhancement in the region where repulsive forces cease to be the predominant component of the interaction.

While studies with respect to the power terms (γ_w, γ_r) in Fig. 2(a) provide important information on the nature of the interaction at play in MSAFM, the combination of other parameters such as the driving frequencies ω_{cu} and ω_s and amplitudes a_{cu} and a_s play a major role in the experimental usefulness of the synthesized modes. In Fig. 3 contour plots of a_- as a function of the driving frequencies ω_{cu} and ω_s exhibit a band of frequencies where the amplitude of the signal is higher. The bands correspond to the combination of frequencies matching with the resonance of the flexural modes of the cantilever in contact with the sample. The

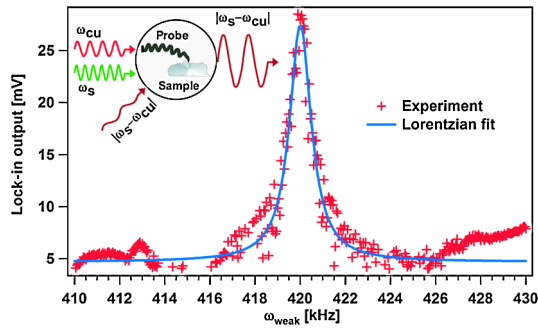


FIG. 4 (color online). Concept and characterization of virtual resonance. The inset depicts the process of frequency difference generation and the subsequent process of oscillation enhancement. The newly formed state is shown to be amplified by exhibiting a resonancelike response when stimulated with a weak applied forcing. The data were obtained for incident driving frequencies $\omega_{cu} = 4.00$ MHz and $\omega_s = 4.42$ MHz yielding a peak $\omega_- = 420$ kHz. When $S(t)$ is used as the input, the ordinate displays the output of the lock-in amplifier with reference to ω_{weak} , which is tuned in the interval of the abscissa.

theoretical result of Fig. 3(b) is indeed in agreement with the experimental data presented in Fig. 3(a) where a soft cantilever ($k = 0.06$ N/m) in contact with mica was used for the measurement.

The studied nanomechanical frequency difference generation via Γ suggests the possibility of considering the coupled materials (probe-substrate) in a state with a frequency ω_- that may be enhanced in a resonant fashion. Remarkably, we can demonstrate the feasibility of this virtual resonance by invoking a weak incident driving (ω_{weak}) yielding an effective enhancement of the oscillations at ω_- as shown in Fig. 4. Here, a harmonic waveform of amplitude $a_{weak}/a_{cu} = 0.1$ (in general, $a_{weak} \ll a_{cu}, a_s, \dots$) was electronically added to the piezoelectric substrate of the probe, although qualitatively a similar result can be achieved by an addition to the sample's piezoelectric substrate. We note that in this essentially three stimuli system, higher-order couplings (beyond ω_- formation) can occur, which in conjunction with contributions from the mixing of the weak excitation and the higher-order oscillations can give rise to the observed minor spread in the data of Fig. 4. It is evident that such virtual resonance can potentially lead to innovative methodologies in nanometrology.

To summarize, we have shown that within the presented semianalytical model, a number of important dynamical aspects of nanomechanical frequency difference generation can be explored. The nonlinear coupling between the tip of the probe and the surface of the sample in MSAFM exhibits a complex dynamics with tremendous opportunities for nanoscale imaging. While more studies are warranted, such force induced oscillator coupling may potentially be suitable for the detection of embedded nanoscale inhomogeneities enhancing the ability to

noninvasively explore material subsurface for the presence of nanoparticles. The theoretical behavior of the long-range forces is consistent with the experimental observation that the maximum phase change is obtained when the probe is retracted from its original collapse point to the surface. While the coupling is amplified whenever ω_- of the coupled system coincides with a (typically low-lying) resonance ω_c^k of the cantilever, a new enhancement mechanism was demonstrated by introducing the concept of virtual resonance. We have in essence described a process where by using one or several waves of an external elastic field, large effective cross sections for elastic absorption can be attained without the usual requirement of elastic resonance of the oscillator species. Therefore, the applications can be extended to include frequency tuning to create “virtual” resonance conditions in systems lacking prior “real” resonance at a given frequency. The process can be envisioned as atomic collisions, where dipole-dipole coupling between two atoms have been proposed to give rise to new nonlinear optical processes [13].

This research was sponsored by the Oak Ridge National Laboratory (ORNL) BioEnergy Science Center (BESC). The BioEnergy Science Center is a U.S. Department of Energy (DOE) Bioenergy Research Center supported by the Office of Biological and Environmental Research in the DOE Office of Science. ORNL is managed by UT-Battelle, LLC, for the U.S. DOE under Contract No. DE-AC05-00OR22725.

*passianan@ornl.gov

- [1] A. Glinsky, Ph.D. thesis, New York University, 1992.
- [2] Y. R. Shen, *Nature (London)* **337**, 519 (1989).
- [3] L. Tetard, A. Passian, and T. Thundat, *Nature Nanotech.* **5**, 105 (2009).
- [4] L. Tetard, A. Passian, K. T. Venmar, R. M. Lynch, B. H. Voy, G. Shekhawat, V. P. Dravid, and T. Thundat, *Nature Nanotech.* **3**, 501 (2008).
- [5] O. Kolosov and K. Yamanaka, *Jpn. J. Appl. Phys.* **32**, L1095 (1993).
- [6] M. T. Cuberes, H. E. Assender, G. A. D. Briggs, and O. V. Kolosov, *J. Phys. D* **33**, 2347 (2000).
- [7] G. S. Shekhawat and V. P. Dravid, *Science* **310**, 89 (2005).
- [8] S. A. Cantrell, J. H. Cantrell, and P. T. Lillehei, *J. Appl. Phys.* **101**, 114324 (2007).
- [9] J. H. Cantrell and S. A. Cantrell, *Phys. Rev. B* **77**, 165409 (2008).
- [10] R. W. Boyd, *Nonlinear Optics* (Academic, New York, 2002), 2nd ed.
- [11] N. Jalili, *Piezoelectric-Based Vibration Control: From Macro to Micro/Nano Scale Systems* (Springer, New York, 2010).
- [12] M. Ashhab, M. V. Salapaka, M. Dahleh, and I. Mezić, *Nonlinear Dynamics* **20**, 197 (1999).
- [13] S. E. Harris and D. B. Lidow, *Phys. Rev. Lett.* **33**, 674 (1974).